Arrhenius Relationship

$$k_p = A_p \exp(-E_{a,p}/RT) \quad (12)$$

$$k_{nr} = A_{nr} \exp(-E_{a,nr}/RT) \quad (13)$$

$$\log (k_p/k_{nr}) = \log (A_p/A_{nr}) - ((E_{a,p} - E_{a,nr}/2.3RT) \quad (14)$$

$$\log (\phi/(1 - \phi)) \text{ vs. } 1/T$$

$$\text{slope} = -(E_{a,p} - E_{a,nr})/2.3R \quad (15)$$

$$\text{intercept} = \log (A_p/A_{nr}) \quad (16)$$

**Registry No.** $[(\eta^5\text{-}C_5H_5)Fe(\eta^6\text{-}p\text{-}Cl_2C_6H_4)]^+$, 51150-13-1; $[(\eta^5\text{-}C_5H_5)Fe(B)]^+$ (B = $\eta^6$-chlorobenzene), 32965-46-1; $[(\eta^5\text{-}C_5H_5)Fe(\eta^6\text{-}C_6H_6)]^+$, 51364-24-0; $[(\eta^5\text{-}C_5H_5)Fe(\eta^6\text{-tol})]^+$, 32760-28-4; $[(\eta^5\text{-}C_5H_5)Fe(\eta^6\text{-}p\text{-xyl})]^+$, 32731-70-7; $[(\eta^5\text{-}C_5H_5)Fe(\eta^6\text{-mes})]^+$, 32757-50-9; $[(\eta^5\text{-}C_5H_5)Fe(B)]^+$ (B = $\eta^6$-durene), 62971-97-5; $[(\eta^5\text{-}C_5H_5)Fe(\eta^6\text{-PMB})]^+$, 62971-98-6; $[(\eta^5\text{-}C_5H_5)Fe(\eta^6\text{-HMB})]^+$, 54688-69-6; $[(\eta^5\text{-}C_5H_5)Fe(\eta^6\text{-}1,3,5\text{-}(t\text{-Bu})_3C_6H_3)]^+$, 90867-12-2; $[(\eta^5\text{-}C_5H_5)Fe(\eta^6\text{-HEB})]^+$, 71713-62-7; $[(\eta^5\text{-}C_5H_5)Fe(\eta^6\text{-}p\text{-xyl})]CF_3SO_3$, 90867-13-3; $[(\eta^5\text{-}C_5H_5)Fe(\eta^6\text{-}p\text{-xyl})]PF_6$, 34978-37-5; $[(\eta^5\text{-}C_5H_5)Fe(\eta^6\text{-}p\text{-xyl})]AsF_6$, 90867-14-4; $[(\eta^5\text{-}C_5H_5)Fe(\eta^6\text{-}p\text{-xyl})]SbF_6$, 90867-15-5; $[(\eta^5\text{-}C_5H_5)Fe(\eta^6\text{-}p\text{-xyl})]BF_4$, 74176-24-2; $[(\eta^5\text{-}C_5H_5)Fe(\eta^6\text{-tol})]PF_6$, 33435-42-6; $[(\eta^5\text{-}C_5H_5)Fe(\eta^6\text{-tol-}d_8)]PF_6$, 90867-17-7; $[(\eta^5\text{-}C_5H_5)Fe(\eta^6\text{-HEB})]PF_6$, 71713-63-8; $[(\eta^5\text{-}C_5H_5)Fe(\eta^6\text{-HEB})]AsF_6$, 90867-18-8; $[(\eta^5\text{-}C_5H_5)Fe(\eta^6\text{-HEB})]SbF_6$, 90867-19-9; $[(\eta^5\text{-}C_5H_5)Fe(\eta^6\text{-HEB})]BPh_4$, 90867-20-2; $[(\eta^5\text{-}C_5H_5)Fe(\eta^6\text{-HEB})]BF_4$, 90867-21-3; $[(\eta^5\text{-}C_5H_5)Ru(\eta^6\text{-}p\text{-}Cl_2C_6H_4)]PF_6$, 80049-71-4; $[(\eta^5\text{-}C_5H_5)Ru(\eta^6\text{-}C_6H_6)]PF_6$, 72812-91-0; $[(\eta^5\text{-}C_5H_5)Ru(\eta^6\text{-tol})]PF_6$, 78618-95-8; $[(\eta^5\text{-}C_5H_5)Ru(\eta^6\text{-mes})]PF_6$, 72804-52-5; $[(\eta^5\text{-}C_5H_5)Ru(\eta^6\text{-PMB})]PF_6$, 90867-23-5; $[(\eta^5\text{-}C_5H_5)Ru(\eta^6\text{-HMB})]PF_6$, 72804-78-5; $[(\eta^5\text{-}C_5H_5)Ru(\eta^6\text{-}1,3,5\text{-}(t\text{-Bu})_3C_6H_3)]PF_6$, 90867-25-7.

---

Contribution from the Research Institute for Materials, Faculty of Science,
University of Nijmegen, Toernooiveld, 6525 ED Nijmegen, The Netherlands

# Molecular Orbital Analysis of the Bonding in Gold Tertiary Phosphine Clusters and Their $^{197}$Au Mössbauer Spectra

J. W. A. VAN DER VELDEN* and Z. M. STADNIK[†]

*Received August 16, 1983*

Extended Hückel molecular orbital calculations have been used in the analysis of the bonding in some mononuclear gold(I) compounds and in a series of gold clusters with monodentate tertiary phosphines. The nature of the metal–metal bond in gold clusters is discussed in terms of calculated overlap populations, which correlate well with crystallographically determined bond distances. Furthermore, an empirical correlation has been established between the Au(6p) electron population and the $^{197}$Au Mössbauer quadrupole splitting, providing a better understanding of the $^{197}$Au Mössbauer spectra of gold clusters. An explanation is provided for the absence of a separate signal for the central Au atom in the $[Au_9(PPh_3)_8]^{3+}$ and $[Au_8(PPh_3)_7]^{2+}$ clusters.

## Introduction

Extended Hückel molecular orbital (EHMO) calculations on the bare skeletons of the $[Au_6]^{2+}$ and the $[Au_9]^{3+}$ clusters have shown that the Au(6s) orbitals dominate the bonding.[1] The dominant role of the Au(6s) orbitals in the bare gold clusters is caused by (i) the large 6s–6p energy separation, which makes hybridization for gold less attractive as compared with that for Cu, Ag, and other transition metals, and (ii) the strong contraction of the Au(5d) orbitals. These observations induced Mingos[1] and Vollenbroek et al.[2] to carry out Hückel calculations in which only 6s–6s overlaps between adjacent gold atoms were considered. This resulted in a similar energy level ordering as in the EHMO calculation and in a successful prediction of the ionic charge on the bare gold skeletons.[1,2] To study the effect of the coordination of ligands to a bare metal skeleton, also an EHMO calculation was performed on $[Au_6L_6]^{2+}$ (L = tertiary phosphine).[1] One filled atomic orbital (AO) was used per ligand, in correspondence with the lone pair donated by the tertiary phosphine upon coordination. From this calculation it was concluded that coordination of ligands to the bare metal skeleton of the $[Au_6]^{2+}$ cluster favors in-pointing hybridization of the metal orbitals. This result was, however, generalized for the larger centered gold clusters, resulting in strong radial and weak peripheral interactions.

In this report we describe the results of EHMO calculations on some mononuclear Au(I) compounds and a series of gold cluster compounds taking into account for the gold atoms the Au(5d), -(6s), and -(6p) AO's. The phosphine ligands were substituted by $PH_3$ units, taking into account the P(3s), -(3p) and H(1s) AO's (Table I). These calculations give an insight into the metal skeleton bonding. They show the importance of the peripheral interactions vs. the radial interactions in centered gold clusters, which has been a point of discussion.[3] Also the absence of a separate signal for the central gold atom in $[Au_9(PPh_3)_8]^{3+}$ and $[Au_8(PPh_3)_7]^{2+}$ in the $^{197}$Au Mössbauer spectra has been subject to discussion. It has been postulated that for some reason its intensity might be too low to be

**Table I.** Parameters Used in the Extended Hückel Molecular Orbital Calculations

| atom | orbital | Slater exponent ($\zeta$) | $H_{ii}$, eV |
|---|---|---|---|
| H | 1s | 1.00 | −13.60 |
| P | 3s | 1.89 | −18.77 |
| | 3p | 1.63 | −10.12 |
| Cl | 3s | 2.36 | −25.27 |
| | 3p | 2.04 | −13.69 |
| Br | 4s | 2.64 | −24.03 |
| | 4p | 2.26 | −12.35 |
| I | 5s | 2.68 | −20.62 |
| | 5p | 2.32 | −10.45 |
| Au | 6s | 2.60 | −9.22 |
| | 6p | 2.58 | −4.28 |
| | 5d | 6.16 ($\zeta_1$), 0.685 ($c_1$)<br>2.79 ($\zeta_2$), 0.570 ($c_2$) | −10.97 |

---

[†] On leave from the Institute of Physics, Jagiellonian University, Cracow, Poland.

(1) D. M. P. Mingos, *J. Chem. Soc., Dalton Trans.*, 1163 (1976).

(2) F. A. Vollenbroek, J. J. Bour, and J. W. A. van der Velden, *Recl. Trav. Chim. Pays-Bas*, **99**, 137 (1980).

(3) J. J. Steggerda, J. J. Bour, and J. W. A. van der Velden, *Recl. Trav. Chim. Pays-Bas*, **101**, 164 (1982), and references therein.

0020-1669/84/1323-2640$01.50/0

Table II. Overlap Populations Involved in the Gold Skeleton Bonding for a Series of Gold Clusters

| compd | structure[a] | mean overlap popln per Au-Au | no. of significant Au bonds[b] | mean overlap popln per specified Au-Au bond (no. of bonds) radial | peripheral |
|---|---|---|---|---|---|
| $Au_2L_2$ | linear | 0.345 | 1 | | |
| $[Au_3L_3]^+$ | trigonal | 0.201 | 3 | | |
| $[Au_4L_4]^{2+}$ | tetrahedral | 0.149 | 6 | | |
| $[Au_5L_5]^+$ | trigonal bipyramidal | 0.153 | 9 | | |
| $[Au_6L_6]^{2+}$ | octahedral | 0.142 | 12 | | |
| $[Au_7L_7]^+$ | pentagonal bipyramidal | 0.119 | 16 | | |
| $[Au_8L_8]^{2+}$ | idealized[c] | 0.161 | 13 | 0.192 (7) | 0.125 (6) |
| $[Au_8L_7]^{2+}$ | idealized | 0.140 | 16 | 0.178 (7) | 0.111 (9) |
| $[Au_9L_8]^{3+}$ | idealized | 0.127 | 20 | 0.160 (8) | 0.105 (12) |
| $[Au_9L_8]^+$ | idealized | 0.172 | 14 | 0.209 (8) | 0.122 (6) |
| $[Au_{11}L_{10}]^{3+}$ | idealized | 0.118 | 27 | 0.158 (10) | 0.095 (17) |
| $[Au_{13}L_{12}]^{5+}$ | idealized | 0.101 | 42 | 0.127 (12) | 0.091 (30) |

[a] X-ray analyses have provided the structures on which the EHMO calculations have been performed;[3] clusters with two, three, or five gold atoms are hypothetical and have been assigned the most probable structures. [b] As the criterion for significant Au-Au bonding a minimum overlap population of 0.05 was used. [c] See Experimental Section.

detected or that its signal coincides incidentally with that of the peripheral gold atoms.[3] It will be shown that the Au(6p) electron populations can be correlated with the observed quadrupole splittings in the $^{197}$Au Mössbauer spectra. This provides a better understanding of the $^{197}$Au Mössbauer spectra of the gold clusters and gives a good explanation for the absence of a separate signal for the central gold atom in the two above-mentioned clusters.

## Experimental Section

**Calculations.** The molecular orbitals of the mononuclear Au(I) compounds and gold clusters were calculated by means of the LCAO-MO extended Hückel method.[4] The computer program was based on the self-consistent charge method. In this method a set of secular equations of the form

$$\sum_j (H_{ij} - ES_{ij})c_j = 0 \tag{1}$$

is constructed in a semi-empirical wax. The overlap matrix elements $S_{ij}$ defined by

$$S_{ij} = \langle \psi_i | \psi_j \rangle \tag{2}$$

are calculated with the Slater type atomic orbitals $\psi_i$. The Hamiltonian matrix element $H_{ij}$ is defined by

$$H_{ij} = \langle \psi_i | H_{\text{eff}} | \psi_j \rangle \tag{3}$$

where $H_{\text{eff}}$ is an effective one-electron Hamiltonian, which is chosen to be charge dependent, according to

$$H_{ii} = -\alpha_i - k\beta_i q_a - k^2\gamma_i q_a^2 \tag{4}$$

$$H_{ij} = KS_{ij}(H_{ii} + H_{jj})/2 \tag{5}$$

Here $\alpha_i + \beta_i q_a + \gamma_i q_a^2$ is the valence state ionization energy (VSIE) of orbital $\psi_i$, $q_a$ is the Mulliken charge of the atom a on which the orbital $\psi_i$ is centered, and $k\beta_i q_a + k^2\gamma_i q_a$ describes the charge dependency of the VSIE, with $k$ ($k$ = 0-1) as an empirical parameter for the influence of the surrounding atoms. The value of the empirical constant $K$, introduced by Wolfsberg and Helmholz, lies usually between 1.5 and 3.0. Calculations with $k = 0$ and $K = 2.5$ have given results independent of the chosen parameters for $Cu(dtc)_2$,[5] and therefore these values have also been used. With $k = 0$ no iterative calculations are required, which limits the computer time. From atomic spectra $\alpha_i$ can be calculated.[6] Except for the Au(5d) orbitals, which were represented by double-exponent functions, we have used single-exponent Slater orbitals retaining only the term with the highest power of $R$ from the functions given in the literature[7-9] (Table I). All the distances, which were used in the calculations, are the averages of the experimentally found distances for a large series of gold cluster compounds. For all Au-P distances 2.30 Å was used. For all noncentered gold clusters (2-7 Au atoms) Au-Au distances of 2.70 Å were used with idealized structures (Table II). Nearly all centered gold clusters (8-13 Au atoms) are found to have structures that are related to the icosahedron. Therefore, icosahedrally derived structures with uniform radial distances of 2.70 Å and peripheral distances of 2.85 Å have been used, with linear P-Au-$Au_{\text{centr}}$ entities. To limit the calculation time, phosphines were substituted by $PH_3$ units (P-H = 1.42 Å and H-P-H = 104°, which is the C-P-C angle in coordinated $PPh_3$ in gold phosphine clusters).

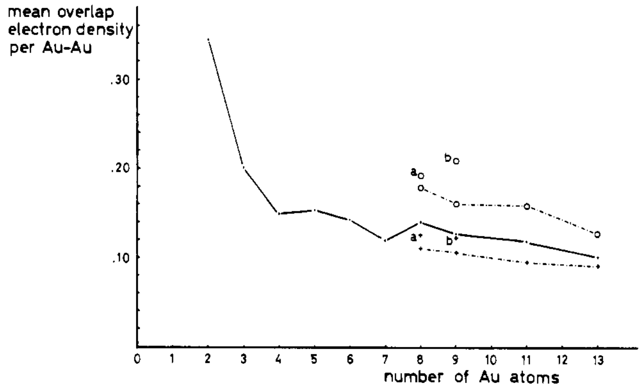

Figure 1. Mean overlap population per Au-Au bond vs. the number of gold atoms in a cluster (see also Table II): (a) $[Au_8L_7]^{2+}$; (b) $[Au_9L_8]^+$. For centered gold clusters mean overlap populations are shown separately for radial (O) and peripheral (+) Au-Au bands.

## Bonding in the Gold Cluster Skeleton

Both Mingos[1] and Vollenbroek et al.[2] have pointed out that the bonding in the metal skeletons of ligand-containing gold clusters is dominated by linear in-pointing Au(s-z) hybrids. In the centered gold clusters (8-13 Au atoms) this results in strong center-to-periphery (or radial) interactions and weak peripheral interactions on the outside of the cluster. However, it will be pointed out that the peripheral interactions are by no means negligible.

In Figure 1 the calculated mean overlap populations per Au-Au bond vs. the number of gold atoms in a cluster are

---

(4) R. Hoffmann, *J. Chem. Phys.*, **39**, 1397 (1963).

(5) C. P. Keijzers, H. J. M. de Vries, and A. van der Avoird, *Inorg. Chem.*, **11**, 1338 (1972).

(6) C. E. Moore, *Natl. Bur. Stand.* (*U.S.*), *Circ.*, **467**: Vol. I (1949), Vol. II (1952), Vol. III (1958); H. Basch, A. Viste, and H. B. Gray, *Theor. Chim. Acta*, **3**, 458 (1965).

(7) J. Richardson, W. Nieuwpoort, R. Powell, and W. Edgell, *J. Chem. Phys.*, **36**, 1057 (1962).

(8) J. Richardson, R. Powell, and W. Nieuwpoort, *J. Chem. Phys.*, **38**, 796 (1963).

(9) E. Clementi and D. Raimondi, *J. Chem. Phys.*, **38**, 2686 (1963).

**Table III.** Overlap Population in $Au_2$ vs. the Interatomic Distance (Å)

| dist | overlap popln | dist | overlap popln |
|---|---|---|---|
| 2.30 | 0.368 | 2.70 | 0.244 |
| 2.40 | 0.336 | 2.80 | 0.216 |
| 2.50 | 0.304 | 2.90 | 0.189 |
| 2.60 | 0.273 | | |

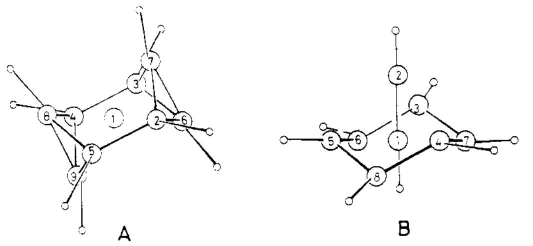

**Figure 2.** Au–P skeletons for (A) $[Au_9L_8]^{3+}$ and (B) $[Au_8L_8]^{2+}$ with numbering schemes.

shown (see also Table II). For $Au_2L_2$ ($L = PH_3$) a maximum value is observed, which decreases continuously with increasing cluster size. This trend, however, does not lead to an increased instability upon cluster growth, since the number of intermetallic bonds increases also very drastically.

To evaluate the relative importance of radial vs. peripheral bonding in centered gold clusters, we have given in Figure 1 and Table II separately the overlap populations for radial and peripheral bonding. It can be noticed that the peripheral bonds are always weaker (65 ± 5% in all calculations) than the radial bonds. This is in agreement with the larger peripheral bond length (2.86 Å) as compared with the radial bond length (2.70 Å). The effect of the bond length upon the overlap population can be judged from calculations on a $Au_2$ dimer (Table III).

It can be seen that the radial and peripheral bond strengths are of comparable magnitude.[1,2] The total overlap population in the peripheral Au–Au bonds relative to the radial Au–Au bond increases rapidly upon cluster growth. This is caused by the rapidly increasing number of neighboring interactions when more gold atoms are added to the periphery. For a $Au_{13}$ cluster this results in almost twice the overlap population in the peripheral network when commpared with that in the radial network.

Therefore, centered gold clusters should be described with strong radial Au–Au interactions. The peripheral Au–Au interactions are of comparable magnitude, but their total overlap population is dominant for the larger clusters.

To establish the validity of the above considerations, the calculated overlap populations and the crystallographically determined bond lengths were compared for two gold phosphine clusters: $[Au_9(P(p\text{-tol})_3)_8]^{3+}$ [10] (tol = tolyl) and $[Au_8(PPh_3)_8]^{2+}$.[2,11] These two were chosen because they represent two structurally different types of centered gold clusters. In the $Au_8$ cluster the central Au atom is bonded to seven Au–phosphine entities and one phosphine. In the $Au_9$ cluster the central Au atom is surrounded by eight gold–phosphine entities, from which four deviate from linearity (150°, see Figure 2). In Table IV a comparison is made between the calculated overlap populations and bond lengths for both compounds. A reasonable correlation can be observed with strong and short radial bonds and somewhat weaker and longer peripheral bonds. Two calculations have been performed on the $Au_9$ cluster, one with only linear P–Au–$Au_{center}$ entities and one with four linear and four bent (150°) entities, but all Au–Au and Au–P distances were kept constant. It is remarkable that the overlap populations between the atoms 6–7 and 8–9 increase, which are the atoms in the bent entities.

**Table IV.** Bond Lengths vs. the Overlap Populations in Au–Au Bonds for $[Au_9L_8]^{3+}$ and $[Au_8L_8]^{2+}$

| compd | bond | overlap popln[a] I | overlap popln[a] II | bond length, Å |
|---|---|---|---|---|
| $[Au_9L_8]^{3+}$ | 1–(2–5) | 0.174 | 0.172 | 2.68 |
| | 1–(6–9) | 0.146 | 0.140 | 2.72 |
| | 6–7, 8–9 | 0.096 | 0.114 | 2.75 |
| | 2–5, 3–4 | 0.117 | 0.112 | 2.79 |
| | all others | 0.104 | 0.106 | 2.87 ± 0.02 |
| $[Au_8L_8]^{2+}$ | 1–2 | 0.252 | | 2.64 |
| | 1–(3–5) | 0.192 | | 2.70 ± 0.01 |
| | 1–(6–8) | 0.173 | | 2.72 ± 0.01 |
| | 5–(6,8), 7–(3,4) | 0.128 | | 2.87 ± 0.03 |
| | 3–6, 4–8 | 0.119 | | 2.86 |
| | 2–(3–5) | 0.022 | | 2.93 ± 0.03 |

[a] Legend: I, idealized structure; II, realistic structure (see text).

In contrast to the $Au_9$ cluster the bonding in the $Au_8$ cluster is quite different, since the radial interactions are dominant not only in strength but also in number as compared to the peripheral interactions (see also Table II). Remarkable is the very strong interaction between Au(2) and the central atom Au(1). This Au(2) shows almost no interactions with other peripheral gold atoms and can be considered to be bonded exclusively to the central gold atom and a phosphine ligand in an exact trans position. This result has also been obtained for the structurally analogous $[Au_9L_8]^+$ and $[Au_{11}L_{10}]^{3+}$.

The overlap population present in the Au–P bond is constant (0.364 (1)). There is, however, one exception: the phosphine bonded to the central gold atom in $[Au_8L_8]^{2+}$ is significantly more weakly bonded (0.307). Structurally this weakness in bonding is expressed in a very long $Au_{centr}$–P bond (2.42 (1) Å) compared with any other Au–P bond in gold triarylphosphine clusters (2.29 (2) Å). Sterical hindrance has been suggested[2] to be a factor in the lengthening of this Au–P bond, but certainly also electronical factors play an important role and weakening could be caused by the strongly bonded Au(2) trans to the phosphine. Chemically its lability could be observed in the reaction

$$[Au_8(PPh_3)_8]^{2+} + {}^1/_4[RhCl(C_8H_{14})_2]_2 \rightarrow [Au_8(PPh_3)_7]^{2+} + {}^1/_4[RhCl(PPh_3)_2]_2 + C_8H_{14}$$

where exclusively the phosphine coordinated to the central gold atom is abstracted.[12]

## Energy Level Ordering

In Figure 3 energy level schemes are shown for a series of gold cluster compounds ranging in size from 2 to 13 gold atoms and also for the metal–phosphine fragment which may be considered as a building block for gold and the platinum-group clusters.[13] For the Au–phosphine fragment the orbitals that have dominant 5d character are practically nonbonding. The orbitals that are dominantly involved in the metal–metal bonding of this fragment are the hybrid (6s-z) and the higher lying degenerate pair of Au($6p_x$) and Au($6p_y$) orbitals.

In describing some trends in the energy level schemes for this series of gold clusters, the following remarks can be made:

(i) Every gold cluster has *one* low-lying totally symmetric MO that is strongly bonding in the Au skeleton and shows a stabilization upon increasing cluster size. This MO is dom-

---

(10) P. L. Bellon, F. Cariati, M. Manassero, L. Naldini, and M. Sansoni, *J. Chem. Soc., Chem. Commun.*, 1423 (1971).

(11) M. Manassero, L. Naldini, and M. Sansoni, *J. Chem. Soc., Chem. Commun.* 385 (1979); F. A. Vollenbroek, W. P. Bosman, J. J. Bour, J. H. Noordik, and P. T. Beurskens, *J. Chem. Soc., Chem. Commun.*, 387 (1979).

(12) J. W. A. van der Velden, J. J. Bour, W. P. Bosman, and J. H. Noordik, *J. Chem. Soc., Chem. Commun.*, 1218 (1981).

(13) P. R. Raithby, "Transition Metal Clusters", B. F. G. Johnson, Ed., Wiley, Chichester, 1980.

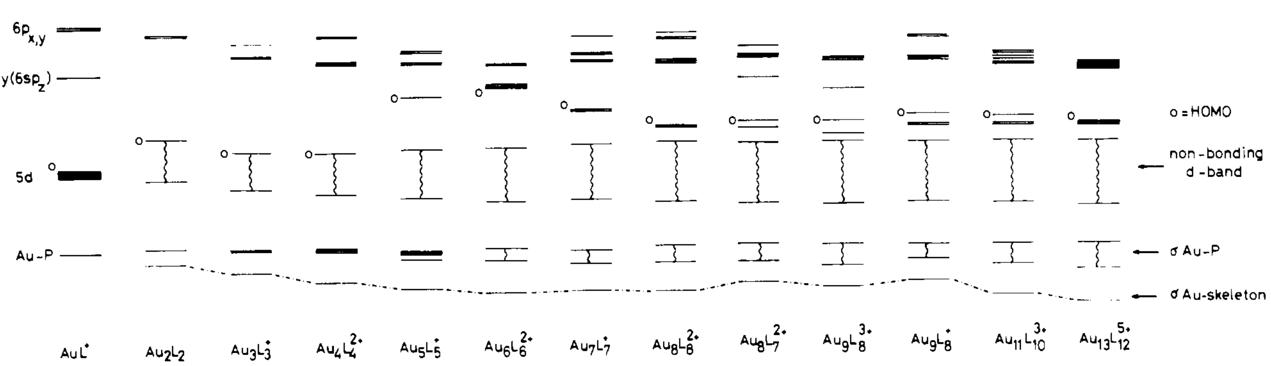

**Figure 3.** Relative energy level scheme for a series of gold cluster compounds and the AuL fragment.

inantly constituted by hybridized Au(6s-5d$_{z^2}$) AO's, where the percentage 5d$_{z^2}$ character decreases from 70% to 15% upon increasing the cluster size from 2 to 13 gold atoms.

(ii) There are $n - 1$ MO$_3$'s representing Au–P $\sigma$ bonds for clusters containing $n$ AuL fragments.

(iii) The following group of $5n + 1$ MO's for a cluster of $n$ gold atoms is essentially nonbonding. These MO's are dominated by Au(5d) orbitals.

(iv) The next levels are either empty or (partly) filled. The weakly bonding MO's arise mainly from $\sigma$ and/or $\pi$ interactions between electrons in Au(5d) and Au(6p) AO's. The number of filled MO's ranges from 0 to 3 on going from 2 to 13 gold atoms.

From the above-mentioned trends it may be concluded that the gold skeleton bonding in gold clusters is mainly determined by a low-lying totally symmetric MO arising from bonding interactions between all gold atoms. Also of importance for the gold skeleton bonding are the highest filled MO's (group iv), since groups ii and iii represent only the gold–ligand interactions and the essentially nonbonding Au(5d) levels. In a comparison of our results with the energy level schemes obtained from the Hückel calculations on the bare gold skeletons[1,2] a similar energy level ordering can be observed when one considers only the MO's involved in the gold skeleton bonding. The present results are supplementary to the EHMO calculations of Evans and Mingos.[22]

## EHMO Calculations and $^{197}$Au Mössbauer Spectroscopy

$^{197}$Au Mössbauer spectroscopy is a technique that can be used successfully to obtain specific information about the electronic properties of the gold atoms in gold clusters. Several reports have shown that the Mössbauer spectra can be interpreted by assuming different gold sites, with parameters that are mainly determined by the ligand present at the particular gold site, while geometrical site differences often have no detectable influence. Thus, for centered gold clusters, the peripheral gold atoms in $Au_{11}(PPh_3)_7X_3$ and $[Au_{11}(PPh_3)_8X_2]^+$ give rise to two quadrupole pairs in their Mössbauer spectra, while those in $[Au_8(PPh_3)_7]^{2+}$, $[Au_8(PPh_3)_8]^{2+}$, $[Au_9(PPh_3)_8]^+$, $[Au_9(PPh_3)_8]^{3+}$, and $[Au_{11}(PPh_2(CH_2)_3PPh_2)_5]^{3+}$ give rise to only one quadrupole pair.[12,14,15] The IS and QS parameters are in the region that is typical for linearly coordinated Au(I) compounds. It has, therefore, been argued that the peripheral gold atoms are seemingly linearly hybridized with one hybrid orbital involved in the bonding of the ligand and the other in the bonding of the gold cluster.[14] The central gold atom in $[Au_8(PPh_3)_8]^{2+}$, $[Au_9(PPh_3)_8]^+$, $Au_{11}(PPh_3)_7X_3$ and $[Au_{11}(PPh_3)_8X_2]^+$ shows up as a singlet in the Mössbauer spectrum. The zero quadrupole splitting (QS) has been ascribed to the almost spherical symmetry of the environment of the central gold atom.

**Table V.** Measured $^{197}$Au Mössbauer Quadrupole Splittings (QS, mm/s) vs. the Asymmetry Parameter $A$ $(=\Sigma_{i=x,y,z}|\bar{E}_{6p} - E_{6p_i}|)$

| compd | Au site | QS | $A$ | no. in plot |
|---|---|---|---|---|
| $Au^ILCl$ | | 7.50 | 0.539 | 1 |
| $Au^ILBr$ | | 7.35 | 0.591 | 2 |
| $Au^ILI$ | | 8.30 | 0.619 | 3 |
| $[AuL_2]^+$ | | 9.46 | 0.755 | 4 |
| $[Au_4(\mu\text{-}Au)_2L_8]^{2+}$ | $Au_4$ | 7.0 | 0.597 | 5a |
| | $(\mu\text{-}Au)_2$ | 7.2 | 0.654 | 5b |
| $[Au_7L_7]^+$ | axial | 4.1 | 0.181 | 6a |
| | equatorial | 6.9 | 0.592 | 6b |
| $[Au_8L_8]^{2+}$ | central | 0 | 0.068 | 7a |
| | peripheral | 6.7 | 0.357 | 7b |
| $[Au_8L_7]^{2+}$ | central | *a* | 0.399 | 8a |
| | peripheral | 6.9 | 0.399 | 8b |
| $[Au_9L_8]^{3+}$ | central | *a* | 0.326 | 9a |
| | peripheral | 6.6 | 0.385 | 9b |
| $[Au_9L_8]^+$ | central | 0 | 0.089 | 10a |
| | peripheral | 6.8 | 0.362 | 10b |
| $[Au_{11}L_{10}]^{3+}$ | central | 0 | 0.044 | 11a |
| | peripheral | 6.6 | 0.288 | 11b |
| $[Au_{13}L_{12}]^{5+}$ | central | *b* | 0.001 | |
| | peripheral | *b* | 0.247 | |
| $Au_4L_4(\mu\text{-}I)_2$ | | 6.5 | 0.442 | 12 |

[a] Not observed as a separate signal. [b] Not measured.

It has always been puzzling, however, that, for the structurally related $[Au_9(PPh_3)_8]^{3+}$ and $[Au_8(PPh_3)_7]^{2+}$, no separate signal could be detected for the central gold atoms. As the quadrupole splitting is caused by a nonsymmetric charge distribution, it is mainly determined by a nonspherical electron population of the Au(6p) orbitals in these clusters. The electron population in the Au(5d) levels is practically spherical and constant in all calculations and will have no great effect on the quadrupole splitting. An increase in the asymmetry in the Au(6p) electron population should result in an increase in the quadrupole splitting. A clear treatise on the relationship between the electric field gradient and the net populations of the atomic orbitals have been given by de Vries et al.[16] QS can be calculated by using the EHMO program described in the Experimental Section. However, due to the inaccuracy of the input parameters—especially $\langle r^{-3}\rangle$ of Au(6p)[17]—the reliability of the results of these calculations is poor. We therefore make a simplification by introducing an asymmetry factor $A$, defined as

$$A = \sum_{i=x,y,z} |\bar{E}_{6p} - E_{6p_i}|$$

where $E_{6p}$ represents the net population in a Au(6p) orbital. The larger the sum of the absolute differences between the mean and individual net population in the Au(6p) orbitals,

---

(14) F. A. Vollenbroek, J. W. A. van der Velden, J. J. Bour, and J. M. Trooster, *Recl. Trav. Chim. Pays-Bas*, **100**, 375 (1981).

(15) F. A. Vollenbroek, J. J. Bour, J. M. Trooster, and J. W. A. van der Velden, *J. Chem. Soc., Chem. Commun.*, 907 (1978).

(16) J. L. K. F. de Vries, C. P. Keijzers, and E. de Boer, *Inorg. Chem.*, **11**, 1343 (1972).

(17) M. O. Faltens and D. A. Shirley, *J. Chem. Phys.*, **53**, 4249 (1970).

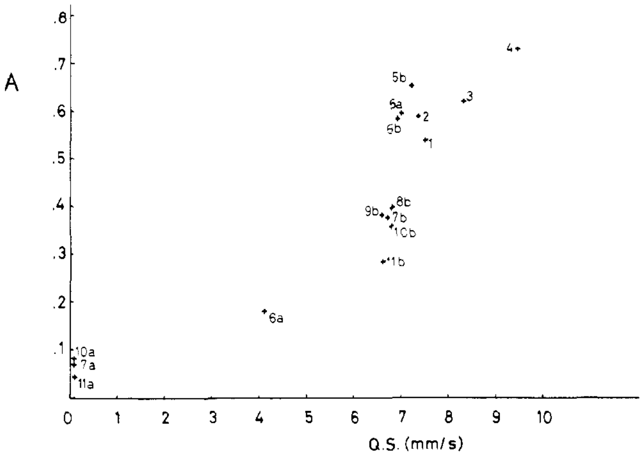

**Figure 4.** QS versus $A$ ($=\sum_{i=x,y,z}|\bar{E}_{6p} - E_{6p_i}|$) for some Au(I) compounds and gold clusters.

the larger will be the electric field gradient on a Au atom.

In Figure 4 (see also Table V) $A$ is plotted against QS and the following observations can be made:

(i) The Au(I) compounds lie in the range with largest QS and $A$ which reflects the linear coordination geometry in these compounds.

(ii) For the so-called centered gold clusters the following things can be observed: (a) the *peripheral* gold atoms occupy a restricted area with lower QS and $A$, indicating a decrease in linear character compared with that of the Au(I) compounds and therefore reflecting the peripheral interactions. (b) The *central* gold atoms in $Au_{11}$, $[Au_9(PPh_3)_8]^+$, and $[Au_8(PPh_3)_8]^{2+}$ have a very small $A$ and zero QS, which implies an almost equal population of the Au(6p) orbitals. As has been formulated in the section on overlap populations, these clusters are structurally related, showing indeed a spherical symmetry for the central gold atom. In contrast, $A$ for the central gold atom in $[Au_9(PPh_3)_8]^{3+}$ and $[Au_8(PPh_3)_7]^{2+}$ is rather large and quite *comparable* to those of the *peripheral* gold atoms, providing an explanation for the fact that no separate signal could be observed for the central gold atoms in these two clusters: the quadrupole pairs for the central and peripheral gold atoms coincide.

(iii) Three other gold clusters that are of interest are the pentagonal-bipyramidal $[Au_7(PPh_3)_7]^+$,[18] the bridged tetrahedral $[Au_4(\mu\text{-}Au)_2(PPh_2(CH_2)_3PPh_2)_4]^{2+}$,[19] and the iodine-bridged $Au_4(PPh_3)_4(\mu\text{-}I)_2$,[20] whose crystal structures have been determined recently (numbers 5, 6, and 12 in Figure 4 and Table V). The Mössbauer spectrum of the first consists of two quadrupole pairs, which could be assigned to the axial and the equatorial gold atoms. The calculations show that the equatorial gold atoms have a large $A$ in accordance with the observed large QS, behaving almost as linear Au(I) compounds. The axial gold atoms, however, have a small asymmetry factor and a small QS but larger parameters than, for example, a central gold atom in the icosahedral $Au_{13}$ cluster, to which it is structurally related. The calculations on the Au-bridged $[Au_4(\mu\text{-}Au)_2L_8]^{2+}$ (L = $PH_3$) show comparable $A$'s for the two gold sites in this cluster, which agrees with the observed quadrupole splittings. This seems strange at first sight, since analogously to Au(I) compounds a large difference would be expected for gold atoms bonded to one or two phosphino groups. This indicates that results obtained from the Mössbauer spectra of Au(I) compounds should be handled carefully in comparison with Mössbauer results for gold clusters. Similarly to the equatorial gold atoms in the $Au_7$ cluster and the two gold sites in the $Au_6$ cluster, the gold atoms in $Au_4L_4(\mu\text{-}I)_2$ show a relatively large $A$ when compared with that of the peripheral gold atoms in the centered gold clusters. This should be attributed to the lower connectivity for the gold atoms in these smaller gold clusters.

No correlation has been found between the calculated electron populations and the isomer shift (IS), which is not astonishing in view of the complexity of the factors that determine the electron density at the Au nucleus, such as screening effects and the restrictions of the EHMO method. Empirically, however, a linear correlation has been established between QS and IS for a huge number of Au(I) and Au(III) compounds and also for gold clusters.[14,21]

## Conclusion

EHMO calculations have shown to be useful in obtaining insight in the bonding of the gold skeletons of gold cluster compounds and also in the understanding of the quadrupole splittings observed in the $^{197}$Au Mössbauer spectra. Centered gold cluster compounds should be described as compositions of gold atoms with strong radial Au–Au interactions. The peripheral Au–Au interactions are of comparable magnitude, but their total overlap population is dominant for the larger clusters. Despite the large number of gold atoms that can surround a central gold atom, large differences in Au(6p) electron configurations can occur which can be correlated simply to the observed quadrupole splittings in the $^{197}$Au Mössbauer spectra. An explanation has been found for the absence of a separate signal for the central gold atom of $[Au_9(PPh_3)_8]^{3+}$ and $[Au_8(PPh_3)_7]^{2+}$.

**Acknowledgment.** We thank Professor J. J. Steggerda for his continuous interest and useful discussions; furthermore we are indebted to Professor E. de Boer and Dr. C. P. Keijzers for critically reading the manuscript and making the computer program available. The investigations were partly supported by the Netherlands Foundation for Chemical Research (SON) with financial aid from the Netherlands Organization for the Advancement of Pure Research (ZWO).

**Registry No.** $[Au_9(PPh_3)_8]^{3+}$, 60477-23-8; $[Au_8(PPh_3)_7]^+$, 74245-04-8; $[Au_9(P(p\text{-}tol)_3)_8]^{3+}$, 59200-55-4; $[Au_8(PPh_3)_8]^{2+}$, 72187-44-1; $[Au_9(PPh_3)_8]^+$, 84623-15-4; $[Au_{11}(PPh_2(CH_2)_3PPh_2)_5]^{3+}$, 80620-23-1; $[Au_4(\mu\text{-}Au)_2(PPh_2(CH_2)_3PPh_2)_4]^{2+}$, 83060-78-0; $Au_4(PPh_3)_4(\mu\text{-}I)_2$, 78519-63-8; $[RhCl(C_8H_{14})_2]_2$, 12279-09-3; Au, 7440-57-5.

---

(18) J. W. A. van der Velden, P. T. Beurskens, J. J. Bour, W. P.; Bosman, J. H. Noordik, M. Kolenbrander, and J. A. K. M. Buskes, *Inorg. Chem.*, in press.

(19) J. W. A. van der Velden, J. J. Bour, J. J. Steggerda, P. T. Beurskens, M. Roseboom, and J. H. Noordik, *Inorg. Chem.*, **21**, 4321 (1982).

(20) F. Demartin, M. Manassero, L. Naldini, R. Ruggeri, and M. Sansoni, *J. Chem. Soc., Chem. Commun.*, 222 (1981).

(21) M. P. A. Viegers, Ph. D. Thesis, University of Nijmegen, Nijmegen, The Netherlands, 1976.

(22) D. G. Evans and D. M. P. Mingos, *J. Organomet. Chem.*, **232**, 171 (1982).